Author's personal copy

2012 Portugal
sl 11/2019

J. Chem. Thermodynamics 47 (2012) 362–371

Contents lists available at SciVerse ScienceDirect

J. Chem. Thermodynamics

journal homepage: www.elsevier.com/locate/jct

Solubility of nicotinic acid in water, ethanol, acetone, diethyl ether, acetonitrile, and dimethyl sulfoxide

Elsa M. Gonçalves [a,b], Manuel E. Minas da Piedade [a,*]

[a] Departamento de Química e Bioquímica, Faculdade de Ciências, Universidade de Lisboa, 1749-016 Lisboa, Portugal
[b] Instituto Politécnico de Setúbal, ESTBarreiro, Rua Américo da Silva Marinho, 2839-001 Lavradio, Portugal

ARTICLE INFO

Article history:
Received 3 October 2011
Received in revised form 12 November 2011
Accepted 14 November 2011
Available online 26 November 2011

Keywords:
Pyridine-3-carboxylic acid
Nicotinic acid
Niacin
Solubility
Activity coefficients
Calorimetry

ABSTRACT

The mole fraction equilibrium solubility of nicotinic acid in six solvents (water, ethanol, dimethyl sulfoxide, acetone, acetonitrile and diethyl ether) differing in polarity, polarizability, and hydrogen-bonding ability, was determined over the temperature range (283 to 333) K, using the gravimetric method. The results obtained led to the solubility order dimethyl sulfoxide (DMSO) ≫ ethanol > water > acetone > diethyl ether > acetonitrile. An analysis based on various solvent descriptors, indicated that this trend seems to be mainly determined by the polarity and polarizability of the solvent. The activity coefficients of nicotinic acid in the different solvents, under saturation conditions, were determined as a function of the temperature and it was found that DMSO exhibits enhanced solubility relative to an ideal solution while the opposite is observed for all other solvents. Both the solvent and the fact that nicotinic acid is primarily zwitterionic in aqueous solution and non-zwitterionic in non-aqueous media, did not affect the nature of the solid phases in equilibrium with the different solutions. Indeed, X-ray powder diffraction, Fourier transform infrared spectroscopy, scanning electron microscopy, and differential scanning calorimetry analysis indicated that, despite some differences in particle size and morphology, the starting material and the solid products obtained at the end of the solubility studies in the six solvents used in this work were all crystalline and corresponded to the same monoclinic phase.

© 2011 Elsevier Ltd. All rights reserved.

1. Introduction

Nicotinic acid (figure 1, CAS number [59-67-6]), pyridine-3-carboxylic acid, is credited to have been synthesized for the first time by Huber, in 1867, via the oxidation of nicotine with sulfuric acid and potassium dichromate (thus the name nicotinic acid) [1]. The compound gained considerable attention over the years because of its versatility in terms of chemical applications and significant biochemical and therapeutic roles. Noteworthy examples of diverse chemical applications are the preparation of matrixes for matrix-assisted laser desorption ionization (MALDI) mass spectrometry analyses of large polypeptides [2]; the uses in zinc electroplating and as an anti-corrosion agent for aluminum–zinc alloys in contact with acid solutions [3]; and the recommendation as a reference material for combustion calorimetry [4,5]. The vitamin function of nicotinic acid (vitamin B_3, commercially known as niacin) [6,7], was demonstrated in the early 20th century [1,8], when it was recognized that its dietary deficiency could lead to the development of pellagra, a disease characterized by a severe photosensitive dermatitis and, ultimately, resulting in dementia and death [9]. This finding subsequently led to the widespread use of nicotinic acid as an additive in food, forage, and cosmetics [7,10].

Nicotinic acid has also been employed since the 1950s, to lower plasma levels of triglyceride (fat) and low density lipoprotein cholesterol (LDL-c) particles (“bad cholesterol”) while concomitantly raising the levels of (“good”) high-density lipoprotein cholesterol (HDL-c) [8,10–13]. It is, in fact, claimed to be the most effective agent currently marketed for raising HDL-c plasma levels [12] and has been extensively explored in the production of drugs for the prevention of atherosclerosis and the risk of cardiovascular events [10,13–15].

Nicotinic acid is solid at ambient temperature and pressure and it is normally purified by crystallization. In general, for the adequate design of processes and products based on cooling crystallization, the solubility of the material of interest in different solvents must be known as a function of temperature, since it is closely related to the maximum achievable yield of solid [16].

Ideally, solubility determinations should always be accompanied by the characterization of the crystal forms in contact with the solution, because phase transitions and solvate formation may occur in the temperature range of the measurements. Moreover, due to variations in solvent–solute interactions, each solvent can stabilize a different type of pre-nucleation aggregate and this may lead to the precipitation of different crystalline forms of the

* Corresponding author. Tel.: +351 217500866; fax: +351 217500088.
E-mail address: memp@fc.ul.pt (M.E. Minas da Piedade).

0021-9614/$ - see front matter © 2011 Elsevier Ltd. All rights reserved.
doi:10.1016/j.jct.2011.11.023

Author's personal copy

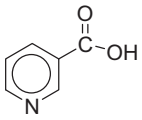

FIGURE 1. Molecular structure of pyridine-3-carboxylic acid (nicotinic acid, NA).

same substance (polymorphs or solvates) [16–18]. Because crystallization always requires some degree of super-saturation – a metastable state – these forms do not, necessarily, correspond to the most thermodynamically stable one. The presence of kinetic barriers can delay, or hinder, the transformation of metastable forms into the most thermodynamically stable one and, hence, metastable polymorphs may result from crystallization processes. Different polymorphs often exhibit significantly different physical properties, such as the fusion temperature, solubility, or the dissolution rate in a given media [19–21]. Hence, overlooking the identification and tight control of polymorph or solvate formation can play havoc with the safe and effective use of a product [19–21].

Here we report the temperature dependence of the solubility of nicotinic acid in six solvents that differ in polarity, polarizability, and hydrogen-bonding ability: water and ethanol (polar and protic); dimethyl sulfoxide (DMSO), acetone, and acetonitrile (polar and aprotic); and diethyl ether (apolar and aprotic). The main objective was to investigate how the solvent nature influenced (i) the solubility of nicotinic acid and (ii) the structural and morphological features of the solid material present in equilibrium with the solution. Also of interest was (iii) the evaluation of how the energetics of these solid materials reflected their structural and morphological differences. The solid products resulting from the solubility experiments were, therefore, compared with the starting material in terms of crystal structure and morphology, by using X-ray powder diffraction and scanning electron microscopy (SEM), respectively, and on energetic grounds by solution and differential scanning calorimetry (DSC). To our knowledge, in addition to some early studies involving water, aqueous NaCl, and 96% (v/v) ethanol [22,23], modern determinations of the temperature dependence of the solubility of nicotinic acid have only been carried out for water and 3-picoline or their mixtures [24]. In none of these cases was the nature of the solids in equilibrium with the solutions evaluated.

The present work is part of a systematic thermodynamic investigation of nicotinic acid and some of its derivatives that was recently started in our laboratory due to the importance of this family of compounds as active pharmaceutical ingredients and food additives. The completed studies have up to now addressed (i) the relationship between structure and thermodynamic stability of both the isolated molecules and anhydrous or hydrate crystal forms of nicotinic acid, 2-, 4-, 5-, and 6-hydroxy nicotinic acids, and 5-chloro-6-hydroxynicotinic acid [25–27]; (ii) the concentration dependence of the enthalpy of solution of nicotinic acid in water [28]; (iii) the influence of temperature and ionic strength on the acidity constants of nicotinic acid in aqueous solution [29], and (iv) the determination of the standard molar enthalpies of formation of the three nicotinic acid species involved in aqueous protonation/deprotonation equilibria at infinite dilution [28].

2. Materials and methods

2.1. General

Infrared spectra were recorded over the range (400 to 4000) cm^{-1} in a Nicolet 6700 Fourier-transform spectrometer, calibrated with polystyrene film. The resolution was 2 cm^{-1}. The samples consisted of translucent pellets prepared by pressing ~1% (w/w) nicotinic acid-KBr powder mixtures in a mechanical press, to ~850 MPa. X-ray powder diffraction (XRPD) analyses were carried out on a Philips PW1730 diffractometer, with automatic data acquisition (APD Philips v.35B), operating in the θ–2θ mode. The apparatus had a vertical goniometer (PW1820), a proportional xenon detector (PW1711), and a graphite monocromator (PW1752). A Cu Kα radiation source was used. The tube amperage was 30 mA and the tube voltage 40 kV. The diffractograms were recorded at $T = (293 \pm 2)$ K in the 2θ range 10° to 40°. Data were collected in the continuous mode, with a step size of 0.015° (2θ), and an acquisition time of 1.5 s per step. The samples were mounted on an aluminum sample holder. The indexation of the powder patterns was performed using the program Chekcell [30]. Scanning electron microscopy (SEM) images of Au/Pd-sputtered samples were recorded in high vacuum, using a FEI ESEM Quanta 400 FEG apparatus, with a resolution of 2 nm. The electron beam voltage was set to 10 kV. GC–MS experiments were performed on an Agilent 6890 gas chromatograph equipped with a HP-5 column (5% diphenyl/95% dimethylpolysiloxane; 28.7 m × 0.25 μm I.D., 250 μm film thickness) and an Agilent 7683 automatic liquid sampler coupled to an Agilent 5973 N quadrupole mass selective detector.

2.2. Materials

The nicotinic acid sample used as starting material for the solubility determinations was the same employed in previous calorimetric and pK_a studies [28,29]. It was obtained by sublimation of a commercial material (Acrös, mass fraction: 0.995) at $T = 393$ K and $p = 1.33$ Pa. The compound had been characterized in terms of chemical purity, phase purity, and morphology by elemental analysis, diffuse reflectance infrared Fourier-transform (DRIFT) spectroscopy, ^{1}H and ^{13}C NMR, GC–MS, XRPD, SEM, and DSC [28]. These chemical analyses showed no evidence of impurities (mass fraction > 0.999) [28]. No mixtures of phases were also detected by XRPD and DSC (see Section 3 below).

The organic solvents ethanol (Panreac, mass fraction: 0.999), DMSO (Aldrich, mass fraction: 0.999), acetone (Aldrich, mass fraction: 0.998), acetonitrile (Acrös, mass fraction: 0.999), and diethyl ether (Panreac, mass fraction: 0.997), were used as received. The aqueous solubility studies were carried out in distilled and deionized water from a Milli-Q Plus system (conductivity 0.1 $\mu S \cdot cm^{-1}$).

Table 1 summarizes relevant information on the provenance and mass fraction purity of the starting materials used for the solubility determinations.

TABLE 1
Provenance and mass fraction purity of the starting materials used in the solubility studies.

Material	CAS number	Supplier	Mass fraction purity
Pyridine-3-carboxylic acid	59-67-6	Acrös	>0.999[a]
Ethanol	64-17-5	Panreac	0.999[b]
DMSO	67-68-5	Aldrich	0.999[b]
Acetone	67-64-1	Aldrich	0.998[b]
Acetonitrile	75-05-8	Acrös	0.999[b]
Diethyl ether	60-29-7	Panreac	0.997[b]

[a] After purification of the received sample, which had a mass fraction purity of 0.995.
[b] Used as received.

Author's personal copy

2.3. Solubility measurements

Equilibrium solubility determinations were performed over the temperature range (283 to 333) K by the gravimetric method [16,31]. The apparatus is illustrated in figure 2. A suspension of nicotinic acid in ~130 cm^3 of solvent was magnetically stirred (~600 rpm) during 48 h, under nitrogen atmosphere, inside a Schlenk tube like glass cell (1). This type of cell allows, if necessary, studies with air sensitive compounds. The temperature of the solution was maintained constant within ±0.01 K by circulating water from a thermostatic bath (2) through the cell jacket. The bath temperature was controlled by a Julabo MB unit (3) and a HAAKE EK20 immersion cooler (4). The temperature of the nicotinic acid suspension was monitored with a resolution of ±0.01 K by a Labfacility ceramic encapsulated Pt100 sensor (5). The sensor was inserted in the glass well (6) containing Baysilone M350 oil to improve thermal contact and was connected in a four wire configuration to an Agilent HP34901A 20 channel multiplexer adapted to a 6½ digits Agilent HP34970A multimeter (7). This sensor had been previously calibrated against a reference platinum resistance thermometer, calibrated at an accredited facility in accordance to the International Temperature Scale ITS-90. The multimeter scanner supports up to ten independent temperature sensors, so that an identical number of cells (with the thermostated water circulation mounted in series) can be simultaneously operated. At the end of the equilibration period stirring was stopped and a sample of the saturated solution (~3 cm^3) was extracted using a preheated syringe adapted to a micro filter (Whatman Spartan 30/0.45 RC) and a Hamilton 7748-06 stainless steel needle. This aliquot was transferred to a previously weighed glass vial of 10 cm^3 volume, which was weighted a second time when loaded with the solution and a third time after the solution was taken to dryness. The weightings were performed with a precision of ±0.01 mg on a Mettler Toledo XS205 balance. The mole fraction of nicotinic acid in the saturated solutions was computed from:

$$x_{NA} = \frac{M_{Solv}(m_3 - m_1)}{M_{Solv}(m_3 - m_1) + M_{NA}(m_2 - m_3)}, \quad (1)$$

where m_1 is the mass of the empty vial, m_2 is the mass of the vial containing the sample of the solution, m_3 is the mass of the vial plus the solid residue, and M_{NA} and M_{Solv} represent the molar masses of nicotinic acid and solvent, respectively. For all solvents measurements were also carried out both in ascending and descending temperature modes. The 48 h equilibration time was deduced from preliminary experiments carried out at T = 293 K, where the concentration of NA after 2 h, 20 h, 32 h and 48 h was determined. These experiments showed that in all solvents equilibrium was reached in less than 32 h (see supporting information).

2.4. pH measurements

The pHs of the saturated aqueous solutions were determined in separate experiments where, prior to measurements, a nicotinic acid suspension was kept under magnetic stirring for ~48 h, inside a 20 to 90 cm^3 double walled Metrohm 6.1418.220 glass vessel. The temperature was maintained constant to within ±0.02 K, by circulating a water-ethanol mixture (3:1 v/v) from a JULABO F33-ME thermostatic bath, through the jacket of the glass vessel. Temperature measurements, with a resolution of ±0.01 K, were performed by using a Pt100 temperature sensor connected in a four wire configuration to an Agilent 34970A 6½ digits multimeter. This sensor had been previously calibrated as described above for the solubility determinations. The pH measurements were performed with a Radiometer Analytical Red Rod pHC2401 combined pH electrode connected to a PHM240 Radiometer Analytical pH meter. The electrode was calibrated at each temperature by using two standard solutions from Radiometer Analytical: citrate buffer (pH 4.00 ± 0.02 at T = 298.15 K) and phosphate buffer (pH 7.00 ± 0.02 at T = 298.15 K).

2.5. Differential scanning calorimetry (DSC)

The characterization of the samples by differential scanning calorimetry was carried out on a DSC 7 from Perkin Elmer. The experiments were performed at a heating rate of 10 $K \cdot min^{-1}$ over the temperature range (298 to 525) K. The temperature and heat flow scales of the instrument were previously calibrated at the same heating rate with indium (Perkin Elmer; mass fraction: 0.99999; T_{fus} = 429.75 K, $\Delta_{fus}h^o$ = 28.45 $J \cdot g^{-1}$). The nicotinic acid samples, with masses in the range 1.8-13.4 mg, were sealed in air, inside aluminum crucibles, and weighed with a precision of ±1 μg in a Mettler M5 micro-balance. Nitrogen (Air Liquide N45), at a flow rate of 0.5 $cm^3 \cdot s^{-1}$, was used as the purging gas.

2.6. Solution calorimetry

Enthalpies of solution in DMSO were determined using the electrically calibrated isoperibol Thermometric Precision Solution Calorimeter (Model 2225) and experimental procedure previously described [28]. The jacket temperature was maintained at T = 298 K with a stability of ±0.2 mK. A typical experiment involved the dissolution of ~50 mg of nicotinic acid in 100 cm^3 of DMSO.

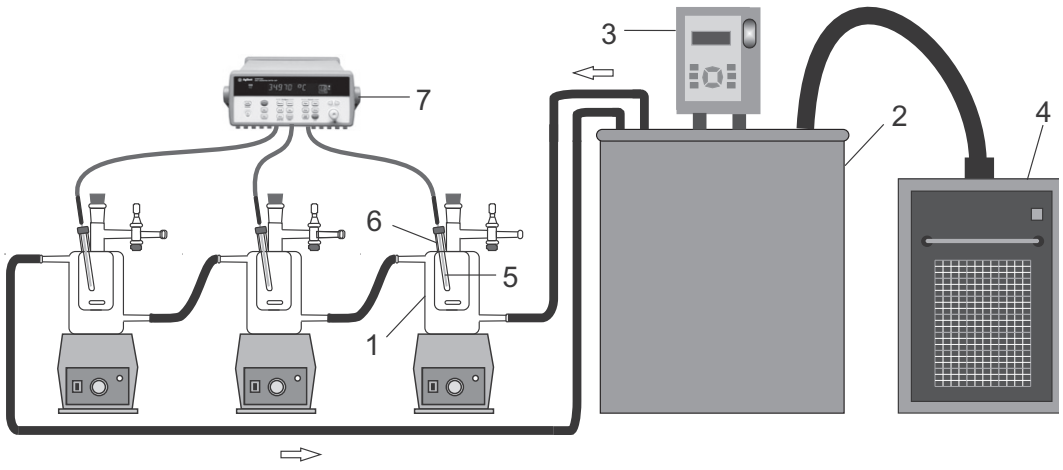

FIGURE 2. Scheme of the apparatus used to determine the solubility of nicotinic acid.

Author's personal copy

The molar enthalpy of the solution process, $\Delta_{sol}H_m$, was calculated from:

$$\Delta_{sol}H_m = -\frac{M}{m}\varepsilon\Delta T_{ad}, \quad (2)$$

where m and M are the mass and the molar mass of the sample, respectively, ε is the calibration constant, and ΔT_{ad} is the corresponding adiabatic temperature change. The values of ΔT_{ad} were derived from the obtained temperature *versus* time curves by using the Regnault–Pfaundler method [32] as implemented in the *SolCal* 1.2 program from Thermometric under the designation dynamics of break. The values of ε correspond to the mean result of two electrical calibrations, one performed before and the other after the solution process, respectively. The heat associated with ampoule breaking was not taken into account, since it was found to correspond to a temperature change of less than 0.1 mK in blank experiments where empty ampoules were broken in 100 cm^3 of water.

2.7. Computational details

Density functional theory (DFT) [33] was applied to predict the dipole moments, polarizabilities, and energetics of the nicotinic acid molecule in different conformations relevant for the discussion of the solubility work here described. Full geometry optimizations and frequency predictions were carried out with the B3LYP [34,35] hybrid functional using the 6-31+G(d,p) [36], basis sets. The calculations were performed with the Gaussian-03 package [37].

3. Results and discussion

All mole fraction quantities were based on molar masses calculated from the standard atomic masses recommended by the IUPAC Commission in 2007 [38].

3.1. Solubility measurements

The results of the solubility determinations in terms of nicotinic acid mole fractions, x_{NA}, are summarized in table 2. The uncertainties quoted correspond to the standard errors of the mean of the number of gravimetric determinations (given in parenthesis) made at each temperature, either on ascending or descending mode. The pHs of the saturated aqueous solutions are also listed.

The x_{NA} against T data in table 2 were fitted to the equation:

$$\ln x_{NA} = a + \frac{b}{(T/K)} \quad (3)$$

by least squares regression. The obtained values of a and b parameters, the determination coefficients (R^2) for 95% probability, and the uncertainties ($\sigma_{\ln x_{NA}}$) assigned to the $\ln x_{NA}$ values computed from equation (3) are listed in table 3. The latter represent standard deviations and were derived from the differences between the corresponding experimental and calculated results.

Plots of the experimental x_{NA} against T data in table 2 and of the corresponding curves based on equation (3) and the parameters in table 3 are compared in figure 3 with the ideal solubility line calculated from equation (6) (see below). Also included in figure 3 are the results previously reported by Wang and Wang [24] for the solubility of nicotinic acid in water and 3-picoline over the temperature ranges (297.15 to 345.05) K and (293.65 to 350.65) K, respectively. The corresponding parameters of equation (3) obtained from the published data are: for water, $a = (2.53468 \pm 0.03728)$, $b = (-2543.98 \pm 12.01)$, $R^2 = 0.9998$, and $\sigma_{\ln x_{NA}} = 6 \cdot 10^{-3}$; for 3-picoline, $a = (2.65791 \pm 0.02807)$, $b = (-1525.20 \pm 9.00)$, $R^2 = 0.9996$, and $\sigma_{\ln x_{NA}} = 4 \cdot 10^{-3}$. The former are in good agreement with the corresponding data obtained in this work, the maximum relative deviation in $\ln x_{NA}$ being <0.5%.

The results in table 2 and figure 3 indicate that the solubility of nicotinic acid varies according to DMSO ≫ ethanol > water > acetone > diethyl ether > acetonitrile. The published mole fraction solubility in 3-picoline [24] exceeds that in DMSO by 1.5% to 2.0% within the same temperature range, the difference decreasing as the temperature increases.

Figure 3 shows that the solubility of nicotinic acid is enhanced in DMSO and 3-picoline and diminished in the remaining solvents relative to ideal solubility. Furthermore, in all cases, x_{NA} smoothly increases with temperature according to equation (3), without any slope variations that could suggest the occurrence of phase transitions or solvate formation. This is also supported by the results of X-ray powder diffraction and Fourier transform infrared spectroscopy analysis (see below), which indicated that both the starting material and the solids obtained at the end of the solubility experiments corresponded to the same monoclinic phase, with no evidence for the presence of polymorphs, mixtures of phases, or solvates.

It is interesting to note that a speciation analysis carried out in the temperature and pH ranges of the solubility experiments in water (table 2) indicated that under those conditions nicotinic acid is primarily (89% to 92%) in a neutral form (see supporting information for details). A neutral form should also be present in non-aqueous media. There is, however, ample experimental and theoretical evidence that in aqueous media this species is predominantly zwitterionic, (A in figure 4) [39–46], while in ethanol [43,47], DMSO [42,44,48] and, presumably, in the other solvents used in this work an equilibrium between conformations B and C in figure 4 is likely to prevail. Calculations at the B3LYP/6-31+G(d,p) level of theory (see supporting information) indicated that, at least for the ideal gas phase, at $T = 298.15$ K, the Gibbs energy of conformation B is smaller than that of conformation C by only 0.99 kJ · mol^{-1}, a value which is very similar to those previously found at the MP2/6-311++G(d,p)//MP2/6-31G(d,p) (1.00 kJ · mol^{-1}) [46], B3LYP/cc-pVTZ (1.03 kJ · mol^{-1}) [25], B3LYP/aug-cc-pVTZ (1.04 kJ · mol^{-1}) [25], B3LYP/6-311++G(d,p) (0.97 kJ · mol^{-1}) [25], G3MP2 (1.06 kJ · mol^{-1}) [25], and CBS-QB3 (1.09 kJ · mol^{-1}) [25]. Based on the above result a Boltzmann distribution analysis indicates that the B ⇄ C system corresponds to an almost equimolar mixture, with $x_{NA,B} = 0.51$ and $x_{NA,C} = 0.49$. This proportion is also likely to hold approximately in solution, at least when dilute solutions are considered. Indeed from published Monte Carlo simulation results [46] it is possible to calculate that in a diluted aqueous solution ($x_{NA} = 0.002$; $x_{H_2O} = 0.998$) the relative mole fractions of species B and C are $x_{NA,B} = 0.52$ and $x_{NA,C} = 0.48$. A similar exercise based on analogous data for dilute methanol solutions ($x_{NA} = 0.004$; $x_{CH_3OH} = 0.996$) [46] leads to $x_{NA,B} = 0.49$ and $x_{NA,C} = 0.51$.

In spite of the different species present in aqueous and non-aqueous media, as mentioned above, the solid phase in equilibrium with the solutions always corresponds to the same monoclinic phase, where the nicotinic acid molecule packs in conformation B of figure 4 [25]. Thus, unlike, for example, its hydroxy derivatives [26], nicotinic acid does not seem to be prone to polymorphism and solvate formation, at least when crystals of the monoclinic $P2_1/c$ phase are initially present in the system. Indeed, albeit a number of co-crystals have been reported, no polymorphs or solvates of nicotinic acid were found in the Cambridge Structural Database [49].

3.2. Materials characterization

Before characterization, all samples resulting from the solubility studies were dried in an oven at $T = 313$ K for ~24 h. The drying

Author's personal copy

TABLE 2
Temperature dependency of the mole fraction (x_{NA}) equilibrium solubilities of nicotinic acid.[a]

Water			Ethanol		DMSO		Acetone		Acetonitrile		Diethyl ether	
T/K	$10^3 \cdot x_{NA}$	pH	T/K	$10^3 \cdot x_{NA}$	T/K	$10^2 \cdot x_{NA}$	T/K	$10^3 \cdot x_{NA}$	T/K	$10^4 \cdot x_{NA}$	T/K	$10^4 \cdot x_{NA}$
283.59	1.721 ± 0.040 (6)	3.604	283.38	2.235 ± 0.004 (3)	293.56	5.966 ± 0.175 (6)	285.46	0.733 ± 0.012 (5)	283.30	0.712 ± 0.168 (7)	283.45	3.224 ± 0.752 (3)
293.41	2.183 ± 0.030 (9)	3.453	293.46	3.087 ± 0.154 (6)	303.38	7.404 ± 0.060 (6)	292.26	1.139 ± 0.026 (9)	288.51	1.204 ± 0.284 (9)	285.74	3.786 ± 0.490 (3)
303.03	2.805 ± 0.076 (5)	3.373	303.15	4.234 ± 0.018 (3)	313.07	9.106 ± 0.085 (5)	296.80	1.373 ± 0.018 (2)	293.01	1.696 ± 0.192 (14)	290.57	5.386 ± 0.486 (3)
312.97	3.655 ± 0.100 (5)	3.273	312.83	6.052 ± 0.078 (3)	322.84	10.852 ± 0.067 (3)	302.14	1.610 ± 0.058 (3)	297.58	1.850 ± 0.148 (9)	294.02	6.179 ± 0.328 (5)
322.83	4.650 ± 0.032 (3)	3.217	322.64	8.427 ± 0.008 (3)	332.36	13.059 ± 0.015 (3)	307.10	2.314 ± 0.066 (4)	302.63	2.680 ± 0.214 (12)	298.66	8.132 ± 0.530 (6)
332.01	5.859 ± 0.052 (3)	3.119	332.43	11.465 ± 0.052 (3)			317.11	3.180 ± 0140 (4)	306.91	3.541 ± 0.158 (6)		
									312.49	4.752 ± 0.200 (9)		
									316.21	5.473 ± 0.166 (6)		
									322.45	7.150 ± 0.342 (6)		
									332.32	10.707 ± 0.300 (3)		

[a] The indicated uncertainties correspond to twice the standard error of the mean of the number of experiments is given in parenthesis.

process did not lead to changes in the morphology or transparency of the crystals, which could indicate the occurrence of a phase transformation or desolvation. Moreover, no contamination by impurities was detected by GC–MS analysis (see supporting information).

The X-ray powder diffractograms collected at $T = (293 \pm 2)$ K for the starting material and all the products obtained at the end of the solubility experiments (see supporting information) could be indexed as monoclinic space group $P2_1/c$. As shown in table 4 the corresponding cell parameters are in good agreement with the single crystal X-ray diffraction results previously reported for the same crystalline phase [49,50].

The conclusion that all samples refer to the same crystalline phase was also corroborated by the results of Fourier transform infrared spectroscopy analysis. As shown in figure 5 the corresponding infrared spectra were very similar, with no evidence of band shifts or other differences that could indicate the presence of distinct polymorphs, solvates, or mixtures of phases.

Scanning electron microscopy imaging (figure 6) indicated that the materials were essentially formed by prismatic crystalline particles, but with significant differences in average size. Image analysis carried out using the Olympus Cell^D 2.6 software led to the Feret's mean diameters, d_F (the mean value of the distance between pairs of parallel tangents to the projected outline of the particle, like in a measurement with a caliper) [51] indicated in table 5. Each value corresponds to the median result for n particles and should be regarded as a very approximate measurement of Feret's mean diameter due to the small number of particles used in the analysis and to the fact that, as show in figure 6, particle superposition/aggregation was impossible to avoid in the SEM imaging.

The DSC measuring curves of both the starting material and the products of the solubility measurements showed only two thermal events over the temperature range (298 to 525) K: a reversible solid–solid phase transition with onset at $T = \sim$453 K and fusion with onset at ~507 K. The temperatures of the peaks onset (T_{on}) and maximum (T_{max}), and the enthalpies of solid–solid phase transition ($\Delta_{trs}H_m$) and fusion ($\Delta_{fus}H_m$) are summarized in table 6, where the uncertainties quoted represent twice the standard error of the mean of four to seven determinations. These results are in good agreement with the analogous data previously reported for a NIST standard reference sample of nicotinic acid (SRM 2151) [25]. The obtained enthalpies of fusion rank amongst the highest published for nicotinic acid ($\Delta_{fus}H_m = 12.4$ kJ · mol^{-1} [52], (13.01 ± 0.32) kJ · mol^{-1} [53], (20.8 ± 0.4) kJ · mol^{-1} [54], 24.6 kJ · mol^{-1} [52], (26.7 ± 0.4) kJ · mol^{-1} [54], 27.57 kJ · mol^{-1} [55], 30 kJ · mol^{-1} [56]), indicating that the samples were significantly crystalline, in agreement with the X-ray powder diffraction evidence. From the baseline shifts observed upon fusion of the products resulting from the solubility measurements in water, ethanol, DMSO, acetone, acetonitrile, and diethyl ether it was possible to calculate the molar heat capacity of fusion of nicotinic acid as $\Delta_{fus}C_{p,m} = (39.6 \pm 3.0)$ J · K^{-1} · mol^{-1} [32]. This value represents the weighted mean [57] of the average results obtained for each of the five different samples. It was assigned to $T = (507.0 \pm 0.4)$ K, which represents the weighted mean of the corresponding T_{on} values. These results are used below to obtain the ideal solubility of nicotinic acid as a function of the temperature. Interestingly, Koop's rule gives for nicotinic acid $\Delta_{fus}C_{p,m}$ (298.15 K) = 38.0 J · K^{-1} · mol^{-1} [58].

The molar enthalpies of solution in DMSO, $\Delta_{sol}H_m$, of the starting material and the products of the solubility measurements, obtained by solution calorimetry, at $T = 298.15$ K, are shown in table 7. Detailed results are given as supporting information. The $\Delta_{sol}H_m$ values correspond to the process:

$$\mathrm{NA(cr)} + 3447\mathrm{DMSO(l)} \rightarrow \mathrm{NA \cdot 3447DMSO(sln)}, \quad (4)$$

Author's personal copy

TABLE 3
Parameters of equation (3), determination coefficients (R^2) and estimated uncertainties ($\sigma_{\ln x_{NA}}$) in the calculation of ln x_{NA}.

Solvent	A	$-b$	R^2	100 $\sigma_{\ln x_{NA}}$
Water	2.04994 ± 0.01833	2394.68 ± 55.67	0.9978	2.4
Ethanol	5.04873 ± 0.27795	3172.75 ± 85.22	0.9971	3.7
DMSO	3.86009 ± 0.06257	1940.57 ± 19.53	0.9997	0.6
Acetone	7.46834 ± 0.82323	4179.00 ± 246.66	0.9863	6.8
Acetonitrile	8.52352 ± 0.58667	5075.54 ± 178.63	0.9902	8.9
Diethyl ether	10.0087 ± 0.81130	5110.31 ± 235.56	0.9937	3.4

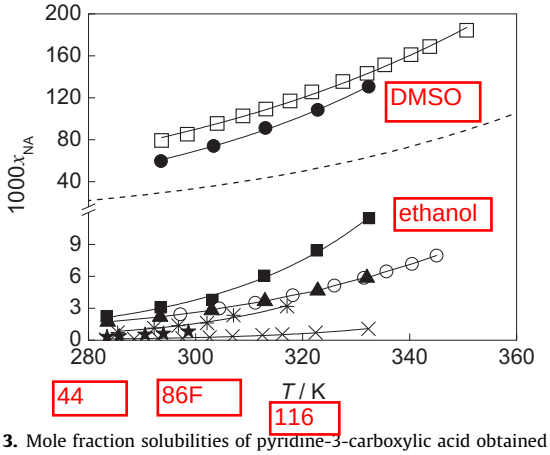

FIGURE 3. Mole fraction solubilities of pyridine-3-carboxylic acid obtained in this work for water (▲), ethanol (■), DMSO (●), acetone (∗), acetonitrile (×), and diethyl ether (★). The open symbols denote data for water (○) and 3-picoline (□), respectively, taken from reference [24]. The dashed line corresponds to the ideal solubility given by equation (6) (see text).

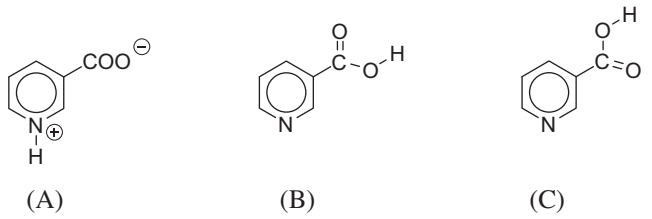

FIGURE 4. Zwitterionic (A) and non-zwitterionic (B and C) neutral molecular conformations of pyridine-3-carboxylic acid.

where on average, (50.1 ± 0.1) mg of each different nicotinic acid sample are dissolved in 100 cm^3 of DMSO (109.574 g; ρ_{DMSO} = 1.09574 g · cm^{-3}) [59] to yield solutions with an approximately identical concentration, corresponding to the mole ratio DMSO/NA = 3447. The uncertainties assigned to $\Delta_{sol}H_m$ represent twice the standard error of the mean of n determinations.

The energetic differences detected by the calorimetric methods do not show any clear correlation with the structural and morphological features of the samples. For example, all other solid state attributes (*e.g.* crystallinity) being constant, the stability of a material is expected to decrease as the particle size becomes smaller, due to the increasing importance of surface *versus* bulk energy [60]. As illustrated in figure 7, the $\Delta_{sol}H_m$ data seem to discriminate between samples originating from protic and aprotic solvents, and the less endothermic $\Delta_{sol}H_m$ value (less stable solid) corresponds to the starting material, which exhibits the smallest particle size (d_F = 1.9 μm). However, the enthalpies of solution of the samples originating from water and ethanol are less endothermic than that of the sample obtained from acetone, despite the fact that the particle size is ~3.5 times smaller in the latter (d_F = 11.3 μm for water, d_F = 11.0 μm for ethanol, and d_F = 3.1 for acetone). In addition, the enthalpy of solution of the product of the solubility studies in DMSO (d_F = 143.8 μm), is equal within the combined uncertainty intervals, to those of the samples corresponding to the remaining aprotic solvents, which exhibit ~16 to 46 times smaller d_F values. This lack of correlation is not totally unexpected. In fact, the X-ray diffraction results indicated that the samples corresponded to the same phase and had no significant differences in crystallinity. Moreover, although the Feret's mean diameters of the samples span a considerably wide range (1.9 μm to 143.8 μm), they are all above the nanometer scale, where a significant influence of size on the particle energetics is likely to occur [60]. Hence, the results in tables 6 and 7 probably reflect the energetic changes resulting from a combination of various small structural and morphological differences (crystallinity, particle size, crystal defects, etc.) without any clear dominant effect from one of them.

TABLE 4
Unit cell parameters (a, b, c, β) and volume (V) obtained by indexation of the powder patterns of the starting material and products of the solubility experiments and corresponding results of single crystal X-ray diffraction (SCXRD) experiments. The data refer to space group $P2_1/c$ and to T = (293 ± 2) K.

Sample or solvent	Unit cell parameters				
	a/nm	b/nm	c/nm	β/°	V/nm^3
SCXRD[a]	0.7186	1.1688	0.7231	113.55	0.5567
Starting material	0.7154	1.1679	0.7228	113.33	0.5545
Water	0.7181	1.1693	0.7220	113.42	0.5563
Ethanol	0.7185	1.1680	0.7228	113.52	0.5563
DMSO	0.7194	1.1641	0.7217	113.39	0.5548
Acetone	0.7185	1.1696	0.7220	113.46	0.5566
Acetonitrile	0.7206	1.1665	0.7221	113.44	0.5569
Diethyl ether	0.7184	1.1669	0.7215	113.48	0.5547

[a] Single crystal X-ray diffraction, references [49,50].

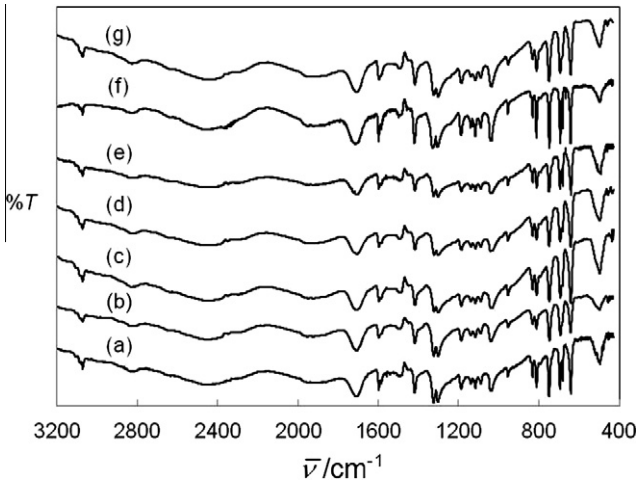

FIGURE 5. Fourier transform infrared spectra of (a) the nicotinic acid sample used as starting material for the solubility studies and of the materials obtained at the end of the experiments in (b) water, (c) ethanol, (d) DMSO, (e) acetone, (f) acetonitrile, and (g) diethyl ether.

3.3. Activity coefficients

The activity coefficients of nicotinic acid, γ_{NA}, in the six solvents studied in this work, at a given temperature along the saturation line, were obtained from:

$$\gamma_{NA} = \frac{x_{NA}^{ideal}}{x_{NA}}, \quad (5)$$

Author's personal copy

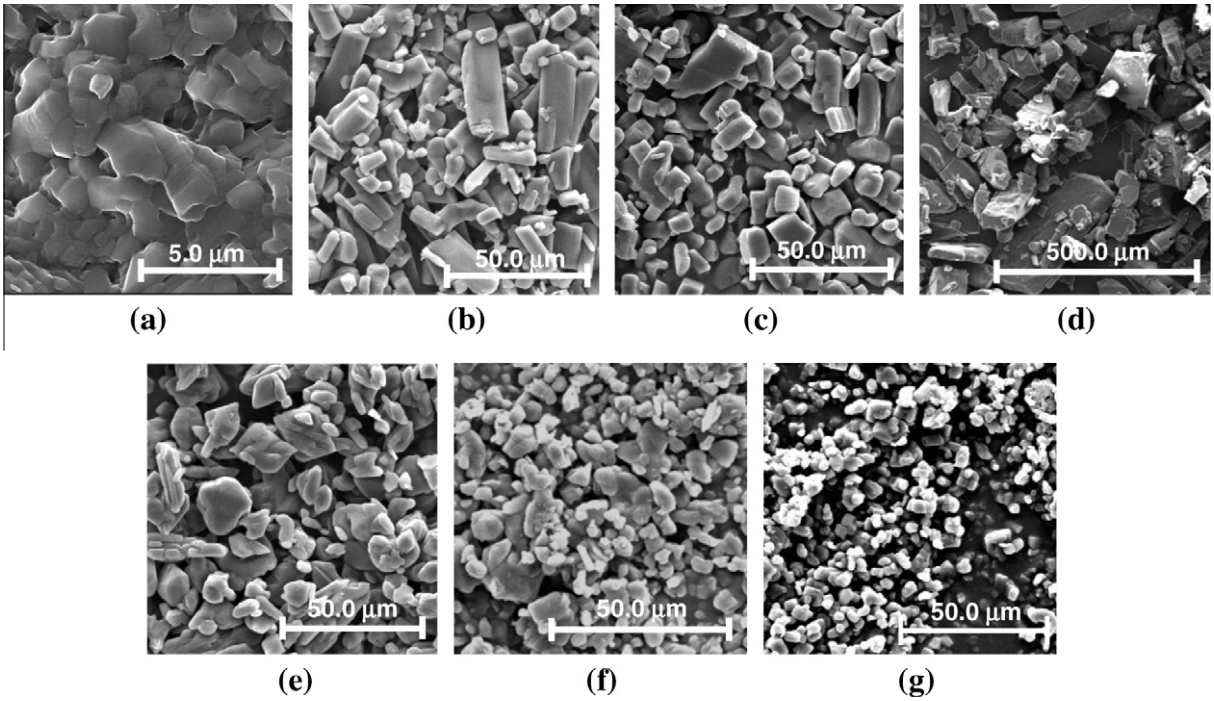

FIGURE 6. SEM images of (a) the nicotinic acid sample used as starting material for the solubility studies and of the materials obtained at the end of the experiments in (b) water, (c) ethanol, (d) DMSO, (e) acetone, (f) acetonitrile, and (g) diethyl ether.

TABLE 5
Feret's mean diameters, d_F, obtained from the analysis of SEM images. Each value corresponds to the median of n measurements.

Sample or solvent	n	d_F/μm
Starting material	48	1.9
Water	81	11.3
Ethanol	90	11.0
DMSO	27	143.8
Acetone	35	3.1
Acetonitrile	55	8.8
Diethyl ether	52	6.6

where x_{NA} is the experimentally determined mole fraction solubility, calculated from equation (3) and the corresponding parameters in table 3, and x_{NA}^{ideal} is the ideal mole fraction solubility given by (see supporting information):

$$\ln x_{NA}^{ideal} = \frac{\Delta_{trs}H_m(T_{trs})}{R}\left(\frac{1}{T_{trs}}-\frac{1}{T}\right)+\frac{\Delta_{fus}H_m(T_{fus})}{R}\left(\frac{1}{T_{fus}}-\frac{1}{T}\right) - \frac{\Delta_{fus}C_{p,m}(T_{fus})}{R}\left(1-\frac{T_{fus}}{T}\right)-\frac{\Delta_{fus}C_{p,m}(T_{fus})}{R}\ln\frac{T_{fus}}{T}. \quad (6)$$

Here, $\Delta_{trs}H_m(T_{trs}) = (1.29 \pm 0.02)\ kJ \cdot mol^{-1}$ is the enthalpy of the solid–solid phase transition observed for nicotinic acid at the temperature $T_{trs} = (453.6 \pm 0.1)\ K$; $\Delta_{fus}H_m(T_{fus}) = (27.7 \pm 0.1)\ kJ \cdot mol^{-1}$ represents the enthalpy of fusion at $T_{fus} = (507.0 \pm 0.4)\ K$; and the term $\Delta_{fus}C_{p,m}(T_{fus}) = (39.6 \pm 3.0)\ J \cdot K^{-1} \cdot mol^{-1}$ is the change in the molar heat capacity of nicotinic acid on fusion mentioned above. These values correspond to weighted means [57] of the onset temperatures, enthalpies, and heat capacities, respectively, of the phase transitions observed by DSC for the products of the solubility studies.

Linear least squares fits of the equation:

$$\ln \gamma_{NA} = A + \frac{B}{(T/K)} \quad (7)$$

to the obtained results over the temperature range (280 to 335) K (see supporting information) led to the A and B coefficients in table 8. Plots of the $\ln \gamma_{NA}$ against $1/T$ data and of the corresponding fitting lines are illustrated in figure 8, which also includes the results obtained from the data on 3-picoline published by Wang and Wang [24] ($A = 2.0397 \pm 0.0364$; $B = -1.0607 \pm 0.0115$; $R^2 = 0.9986$). The enhanced solubility of nicotinic acid relative to an ideal solution is now evidenced in DMSO and 3-picoline by negative values of

TABLE 6
DSC results for the starting material and the products of the solubility studies.

Sample or solvent	n^a	Solid–solid phase transition			Fusion		
		T_{on}/K	T_{max}/K	$\Delta_{trans}H_m$/(kJ · mol^{-1})	T_{on}/K	T_{max}/K	$\Delta_{fus}H_m$/(kJ · mol^{-1})
Starting material	7	453.2 ± 0.3	455.7 ± 0.3	1.03 ± 0.09	507.7 ± 0.6	510.4 ± 0.5	27.6 ± 0.1
Water	5	453.5 ± 0.3	456.5 ± 0.6	1.26 ± 0.08	507.3 ± 0.9	510.1 ± 0.8	27.7 ± 0.1
Ethanol	4	453.3 ± 0.3	455.5 ± 0.4	1.24 ± 0.04	505.3 ± 2.1	509.0 ± 1.6	27.4 ± 0.6
DMSO	5	453.3 ± 0.4	455.7 ± 0.1	1.45 ± 0.08	505.1 ± 1.9	509.4 ± 0.6	27.2 ± 0.3
Acetone	5	453.6 ± 0.1	455.9 ± 0.2	1.34 ± 0.09	507.0 ± 1.0	509.4 ± 0.9	26.8 ± 0.4
Acetonitrile	5	453.6 ± 0.2	455.8 ± 0.4	1.25 ± 0.05	507.3 ± 0.9	509.3 ± 0.7	27.9 ± 0.3
Diethyl ether	5	453.7 ± 0.1	456.0 ± 0.1	1.35 ± 0.05	507.2 ± 0.8	509.7 ± 0.4	27.8 ± 0.2

[a] Number of determinations.

Author's personal copy

TABLE 7
Molar enthalpies of solution, $\Delta_{sol}H_m$, of nicotinic acid in DMSO at $T = 298$ K.

Sample or solvent	n^a	$\Delta_{sol}H_m/(kJ \cdot mol^{-1})$
Starting material	5	19.03 ± 0.08
Water	6	19.59 ± 0.08
Ethanol	8	19.47 ± 0.17
DMSO	5	20.02 ± 0.08
Acetone	5	20.09 ± 0.04
Acetonitrile	5	19.94 ± 0.10
Diethyl ether	6	20.00 ± 0.12

[a] Number of determinations.

$\ln\gamma_{NA} < 0$ ($\gamma_{NA} < 1$) and the corresponding reduced solubility in all other solvents by $\ln\gamma_{NA} > 0$ ($\gamma_{NA} > 1$).

3.4. Solubility trend and the nature of the solvent

As mentioned above the solubility of nicotinic acid in the different solvents used in this work follows the order DMSO ≫ ethanol > water > acetone > diethyl ether > acetonitrile. The possible origin of this trend was analyzed in terms of correlations between $\ln x_{NA}$ at 298.15 K as given by equation (3), and a series of parameters (tabulated for 298.15 K) representative of the polarity, polarizability, and hydrogen bonding (H-bond) characteristics of the solvent. The lack of most of those parameters hindered the extension of the analysis to the published solubility of nicotinic acid in 3-picoline [24]. The selected polarity descriptors were: the dipole moment (μ), Hansen's polar solubility parameter (δ_P) [61], the normalized Dimroth–Reichardt polarity parameter (E_T^N) [61–64], the Grunwald–Winstein solvent polarity parameter (Y) [61–64], and the Kosower polarity parameter (Z) [61–64]. The polarizability descriptors considered were: Hansen's dispersion solubility parameter (δ_D) [61], Hildebrand's solubility parameter (δ), and the molar refractivity (MR) [64]. In addition, the combined Kamlet-Taft dipolarity/polarizability parameter ($\pi*$) was also used [61–63]. Finally, the descriptors related to the H-bond ability of the solvent were the Kamlet-Taft donation (α) and acceptance (β) parameters [61–64], and Hansen's hydrogen bonding solubility parameter (δ_H) [61]. Full details of the methodology of analysis are given as supporting information. In brief, plots of $\ln x_{NA}$ against each individual polarity, polarizability, and H-bond descriptor mentioned above were evaluated by linear least squares regression. The two parameters that gave the best fits in terms of R^2 coefficient were then combined with all remaining descriptors to establish bi-parametric correlations. Only relationships involving independent descriptors were considered. Two descriptors were assumed to be intercorrelated if a linear least squares regression of one against the other led to $R^2 > 0.5$. The significance of the obtained bi-parametric regressions was analyzed in terms of the ANOVA F test. For a 95% confidence level $F = 9.55$ (six data points, three degrees of freedom) [65] and only the bi-parametric correlations with an F test value larger than this limit were judged significant. These corresponded to:

$$\ln x_{NA} = -32.8415 + 1.8417\delta_D - 0.2821\mu, \quad (8)$$

$$\ln x_{NA} = -29.3739 + 1.5682\delta_D - 0.1270\delta_P, \quad (9)$$

with adjusted R^2 coefficients and F parameters of $R^2_{adj} = 0.981$, $F = 131.4$ and $R^2_{adj} = 0.821$, $F = 12.5$, respectively. Because of the limited number of solvents used (six data points) no relationships with more than two parameters were considered.

In principle, a deviation of the results for water from a correlation involving data for other solvents might be observed. Indeed as mentioned above there is ample experimental and theoretical evidence that in aqueous media nicotinic acid is predominantly zwitterionic, A (see figure 4), while in the non-aqueous solvents an equilibrium between species B and C probably exists. Calculations carried out at the B3LYP/6-31+G(d,p) level of theory (see supporting information) indicated that species A-C have similar isotropic polarizabilities (α_0) but considerably different dipole moments and, presumably, different H-bond ability. Specifically, for the zwitterionic form A: $\alpha_0 = 12.5 \cdot 10^{-24}$ cm^3 and $\mu = 14.0$ D; for conformation B: $\alpha_0 = 12.0 \cdot 10^{-24}$ cm^3 and $\mu = 0.71$ D; for conformation C: $\alpha_0 = 12.0 \cdot 10^{-24}$ cm^3 and $\mu = 3.46$ D; and for the equilibrium mixture of forms B and C referred to above ($x_{NA,B} = 0.51$ and $x_{NA,C} = 0.49$): $\alpha_0 = 12.0 \cdot 10^{-24}$ cm^3 and $\mu = 2.06$ D. Although strictly valid for the gas phase this last result will probably not be dramatically changed by solvation effects. Indeed, as stated in section 3.1, the $x_{NA,B}$ and $x_{NA,C}$ values predicted from Monte Carlo simulations in water and methanol are similar to the gas phase ones used above in the calculation of the dipole moment of the B–C mixture. Moreover that result ($\mu = 2.06$ D) is not far from $\mu = 2.48$ D obtained for nicotinic acid in benzene solution [66].

Because of the much larger dipole moment the affinity of the zwitterion for a polar solvent such as water may be expected to be larger than predicted from correlations where the "weight" of the species B–C is larger. Moreover the results of the above mentioned Monte Carlo simulation study indicated that the solvation of the zwitterion relative to species B and C is much more favorable in water than in methanol or tetrahydrofuran [46]. Hence, those correlations should in principle lead to an underestimation of the experimental solubility of nicotinic acid in water. To test this hypothesis, the analogous of equations (8) and (9) obtained from fits where the data for water was ignored were examined. These corresponded to:

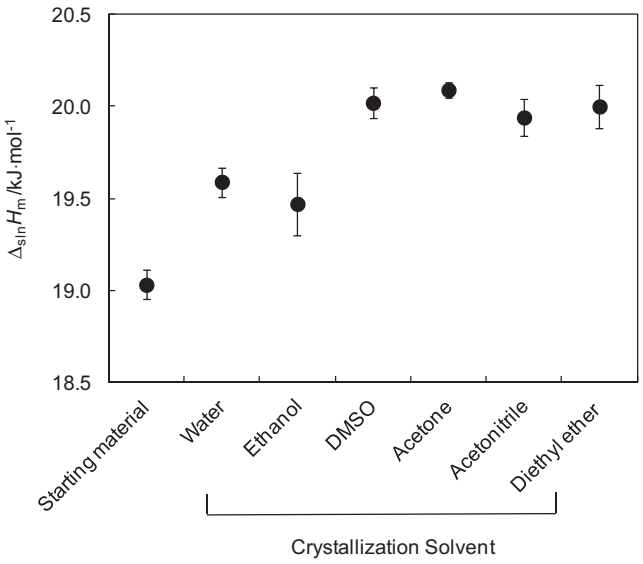

FIGURE 7. Molar enthalpies of solution in DMSO, $\Delta_{sol}H_m$, of the starting material and of the different nicotinic acid products of the solubility studies. The data refer to $T = 298$ K.

TABLE 8
Parameters of equation (7) and determination coefficients (R^2).

Solvent	A	B	R^2
Water	2.4687 ± 0.0365	−0.1357 ± 0.0111	0.9309
Ethanol	−0.5300 ± 0.0365	0.6423 ± 0.0112	0.9967
DMSO	0.7459 ± 0.0343	−0.5974 ± 0.0106	0.9971
Acetone	−3.0634 ± 0.0337	1.6821 ± 0.0101	0.9997
Acetonitrile	−4.005 ± 0.0366	2.5451 ± 0.0112	0.9998
Diethyl ether	−5.7226 ± 0.0264	2.6479 ± 0.0077	0.9999

Author's personal copy

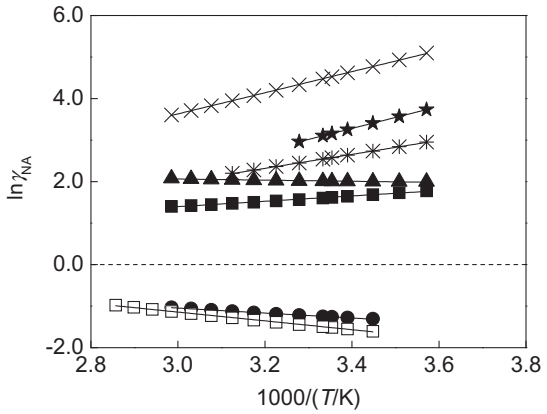

FIGURE 8. Temperature dependence of the activity coefficients of nicotinic acid in water (▲), ethanol (■), DMSO (●), acetone (∗), acetonitrile (×), and diethyl ether (★). The open symbols denote data for 3-picoline (□), taken from reference [24]. The dashed line corresponds to $\gamma_{NA} = 1$ (ideal solubility).

$$\ln x_{NA} = -32.8403 + 1.8393\delta_D - 0.2793\mu, \quad (10)$$

$$\ln x_{NA} = -32.1657 + 1.7758\delta_D - 0.1918\delta_P, \quad (11)$$

with $R^2_{adj} = 0.978$, $F = 89.7$ and $R^2_{adj} = 0.991$, $F = 224.8$, respectively. Both correlations may be considered significant because for five data points and two degrees of freedom the F test limit for 95% confidence level is $F = 19.0$ [65].

Linear least squares regressions to plots of the $\ln x^{calc}_{NA}$ values calculated from equations (8)–(11) against their experimental counterparts $\ln x^{exp}_{NA}$ given by equation (3) led to:

$$\ln x^{calc}_{NA}\ (\text{equation 8}) = (0.989 \pm 0.053)\ln x^{exp}_{NA} - (0.069 \pm 0.334) \quad (R^2 = 0.989), \quad (12)$$

$$\ln x^{calc}_{NA}\ (\text{equation 9}) = (0.893 \pm 0.155)\ln x^{exp}_{NA} - (0.652 \pm 0.980) \quad (R^2 = 0.893), \quad (13)$$

$$\ln x^{calc}_{NA}\ (\text{equation 10}) = (0.989 \pm 0.060)\ln x^{exp}_{NA} - (0.067 \pm 0.386) \quad (R^2 = 0.989), \quad (14)$$

$$\ln x^{calc}_{NA}\ (\text{equation 11}) = (0.996 \pm 0.038)\ln x^{exp}_{NA} - (0.027 \pm 0.245) \quad (R^2 = 0.996). \quad (15)$$

The corresponding line plots are shown in figure 9.

The fact that the best bi-parametric correlations found in this work involve polarity and polarizability descriptors only, suggests that the observed nicotinic acid solubility trend is essentially determined by the combination of these two solvent characteristics. The δ_D–μ correlation does not seem to be sensitive to the different nature of the nicotinic acid species predominating in aqueous and non-aqueous media. As can be seen by comparing equations (12) and (14), in this case, ignoring the data from water does not bring any improvement to the quality of the correlation. Speciation features seem, however, to be captured by the δ_D–δ_P correlation, where the expected underestimation of the experimental solubility of nicotinic acid in water is clearly noted (figure 9b and d). In this case, disregard of the water data leads to a considerable improvement of the correlation, as evidenced by the increase of the determination coefficient from $R^2 = 0.893$ (equation (13)) to $R^2 = 0.996$ (equation (15)).

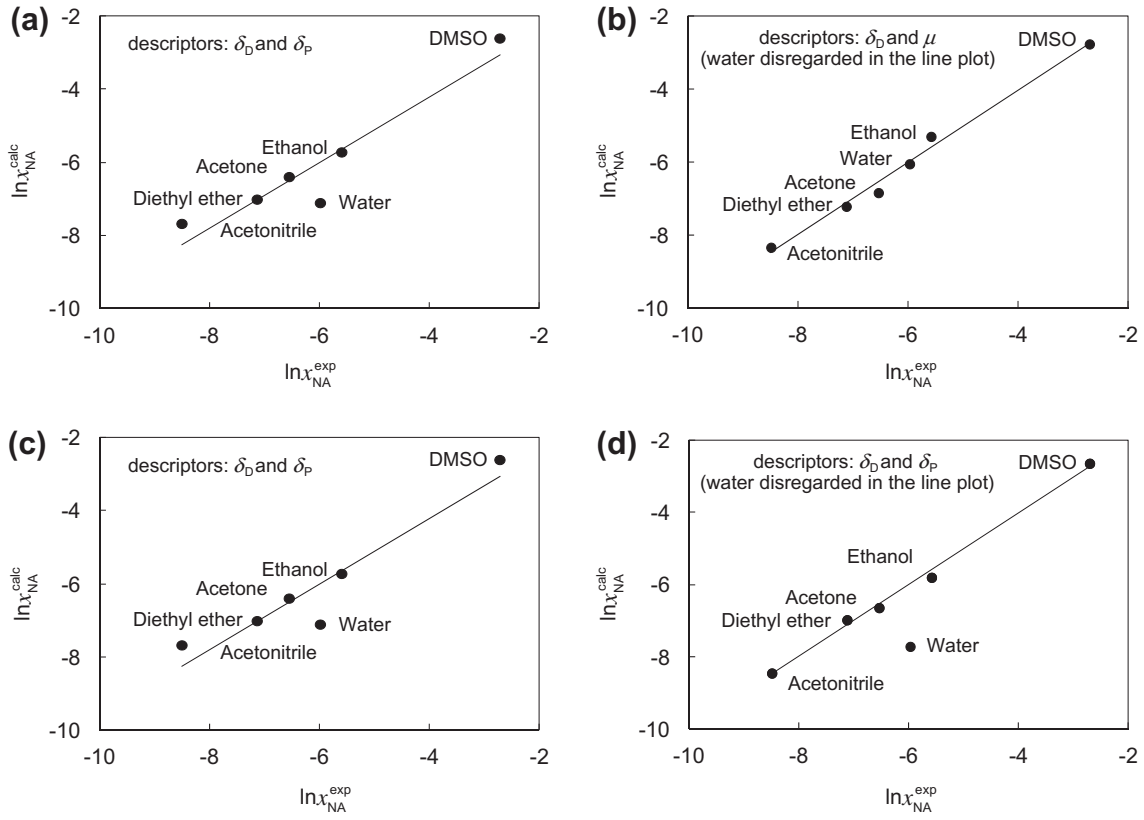

FIGURE 9. Plots of the mole fraction solubility of nicotinic acid calculated, $\ln x^{calc}_{NA}$, from (a) equation (8), (b) equation (9), (c) equation (10) and (d) equation (11), against their experimental counterparts ($\ln x^{exp}_{NA}$). The lines in figures (a) and (b) refer to correlations where data for water was considered – equations (12) and (13), respectively – and those in figures (c) and (d) to correlations where the results for water were disregarded – equations (14) and (15), respectively.

Author's personal copy

4. Conclusions

The results obtained in this study indicate that the solubility of nicotinic acid varies according to DMSO ≫ water > ethanol > acetone > diethyl ether > acetonitrile. This trend seems to be essentially determined by the combined effect of the polarity and polarizability of the solvent.

The solubility of nicotinic acid is enhanced in DMSO and diminished in the remaining solvents relative to ideal solubility.

In all cases, the curves describing the temperature dependence of the solubility smoothly increase with the temperature without any abrupt slope variations that would indicate the presence of phase transitions, mixtures of phases, or solvate formation. This is also supported by the results of X-ray powder diffraction and Fourier transform infrared spectroscopy analysis, which indicated that both the starting material and the solids obtained at the end of the solubility experiments were crystalline and corresponded to the same monoclinic phase ($P2_1/c$). Thus, at ambient pressure, changes in temperature and in the nature of the solvent, and the fact that in water nicotinic acid is predominantly zwitterionic (form A) while in the non-aqueous media an equilibrium between conformations B and C is likely to be present, were not found to induce the initial $P2_1/c$ monoclinic phase to evolve into a different crystalline form.

Acknowledgments

This work was supported by Fundação para a Ciência e a Tecnologia, Portugal (Project PTDC/QUI-QUI/098216/2008). A PhD grant from FCT is gratefully acknowledged by Elsa M. Gonçalves (SFRH/BD/28458/2006). Thanks are also due to Profs. João C.R. Reis and Filomena Martins (FCUL, Portugal) for helpful discussions, Nuno Neng at the laboratory of Prof. José M. Nogueira (FCUL, Portugal) for the performance of the GC–MS analysis, and Daniel Hagmeyer at the group of Prof. Matthias Epple (University of Duisburg-Essen, Germany) for assistance in the recording of the SEM images.

Appendix A. Supplementary data

Supplementary data associated with this article can be found, in the online version, at doi:10.1016/j.jct.2011.11.023.

References

[1] C.A. Elvehjem, L.J. Teply, Chem. Rev. 33 (1943) 185–208.
[2] M. Karas, F. Hillenkamp, Anal. Chem. 60 (1988) 2299–2301.
[3] C. Rio-Estrada, H.W. Dougherty, Vitamins, in: A. Standen (Ed.), Kirk-Othmer Encyclopedia of Chemical Technology, second ed., vol. 21, Wiley, New York, 1970, pp. 509–542.
[4] K.N. Marsh, Recommended Reference Materials for the Realization of Physicochemical Properties, IUPAC–Blackwell Scientific Publications, Oxford, 1987.
[5] R. Sabbah, A. Xu-Wu, J.S. Chickos, M.L. Planas Leitão, M.V. Roux, L.A. Torres, Thermochim. Acta 331 (1999) 93–204.
[6] R. Blum, Vitamins, in: B. Elvers, S. Hawkins (Eds.), Ullmann's Encyclopedia of Industrial Chemistry, fifth ed., vol. A27, VCH, Weinheim, 1996, pp. 581–587.
[7] J. Block, Vitamins, in: S. Seidel (Ed.), Kirk-Othmer Encyclopedia of Chemical Technology, fifth ed, vol. 25, Wiley, Hoboken, 1996, p. 797.
[8] G.A. Goldsmith, J. Am. Med. Assoc. 194 (1965) 167–173.
[9] J. Hegyi, R.A. Schwartz, V. Hegyi, Int. J. Dermatol. 43 (2004) 1–5.
[10] L.A. Carlson, J. Int. Med. 258 (2005) 94–114.
[11] W. Soudijn, I. van Wijngaarden, A.P. Ijzerman, Med. Res. Rev. 27 (2007) 417–433.
[12] P.D. Boatman, J.G. Richman, G. Semple, J. Med. Chem. 51 (2008) 7653–7662.
[13] A. Gille, E.T. Bodor, K. Ahmed, S. Offermanns, Ann. Rev. Pharmacol. Toxicol. 48 (2008) 79–106.
[14] T.L. Lemke, D.A. Williams, V.F. Roche, S.W. Zito, Foye's Principles of Medicinal Chemistry, sixth ed., Lippincott Williams & Wilkins, Baltimore, 2008.
[15] J.J. Li, Triumph of the Heart. The Story of Statins, Oxford University Press, New York, 2009.
[16] J.W. Mullin, Crystallization, fourth ed., Butterworth, Heinemann, Oxford, 2001.
[17] R.J. Davey, N. Blagden, S. Righini, H. Alison, M.J. Quayle, S. Fuller, Cryst. Growth Des. 1 (2001) 59–65.
[18] R.J. Davey, N. Blagden, S. Righini, H. Alison, E.S. Ferrari, J. Phys. Chem. B 106 (2002) 1954–1959.
[19] J. Bernstein, Polymorphism in Molecular Crystals, Oxford University Press, Oxford, 2002.
[20] R. Hilfiker, Polymorphism in the Pharmaceutical Industry, Weinheim, 2006.
[21] H.G. Brittain, Polymorphism in Pharmaceutical Solids, second ed., Informa Healthcare, New York, 2009.
[22] Y.M. Slobodin, M.M. Goldman, Zh. Prikl. Khim. 21 (1948) 859–861.
[23] S.H. Yalkowsky, Y. He, P. Jain, Handbook of Aqueous Solubility Data, second ed., CRC Press, Boca Raton, 2010.
[24] L.C. Wang, F.A. Wang, J. Chem. Eng. Data 49 (2004) 155–156.
[25] E.M. Gonçalves, C.E.S. Bernardes, H.P. Diogo, M.E. Minas da Piedade, J. Phys. Chem. B 114 (2010) 5475–5485.
[26] R.C. Santos, R.M.B.B.M. Figueira, M.F.M. Piedade, H.P. Diogo, M.E. Minas da Piedade, J. Phys. Chem. B 113 (2009) 14291–14309.
[27] E.P. Matias, C.E.S. Bernardes, M.F.M. Piedade, M.E. Minas da Piedade, Cryst. Growth Des. 11 (2011) 2803–2810.
[28] E.M. Gonçalves, T.S. Rego, M.E. Minas da Piedade, J. Chem. Thermodyn. 43 (2011) 974–979.
[29] E.M. Gonçalves, A. Joseph, A.C.L. Conceição, M.E. Minas da Piedade, J. Chem. Eng. Data 56 (2011) 2964–2970.
[30] J. Laugier, B. Bochu, Chekcell. <http://www.ccp14.ac.uk/tutorial/lmgp/chekcell.htm>.
[31] P. Correia, C. Lopes, M.E. Minas da Piedade, J.A.A. Lourenço, M.L. Serrano, J. Chem. Eng. Data 51 (2006) 1306–1309.
[32] J.A. Martinho Simões, M.E. Minas da Piedade, Molecular Energetics, Oxford University Press, New York, 2008.
[33] W. Koch, M.C.A. Holthausen, Chemist's Guide to Density Functional Theory, second ed., Wiley-VCH, Weinheim, 2002.
[34] A.D. Becke, J. Chem. Phys. 98 (1993) 5648–5652.
[35] C. Lee, W. Yang, R.G. Parr, Phys. Rev. B 37 (1988) 785–789.
[36] M.J. Frisch, J.A. Pople, J.S. Binkley, J. Chem. Phys. 80 (1984) 3265–3269.
[37] M.J. Frisch, G.W. Trucks, H.B. Schlegel, G.E. Scuseria, M.A. Robb, J.R. Cheeseman, J.A. Montgomery Jr., T. Vreven, K.N. Kudin, J.C. Burant, J.M. Millam, S.S. Iyengar, J. Tomasi, V. Barone, B. Mennucci, M. Cossi, G. Scalmani, N. Rega, G.A. Petersson, H. Nakatsuji, M. Hada, M. Ehara, K. Toyota, R. Fukuda, J. Hasegawa, M. Ishida, T. Nakajima, Y. Honda, O. Kitao, H. Nakai, M. Klene, X. Li, J.E. Knox, H.P. Hratchian, J.B. Cross, C. Adamo, J. Jaramillo, R. Gomperts, R.E. Stratmann, O. Yazyev, A.J. Austin, R. Cammi, C. Pomelli, J.W. Ochterski, P.Y. Ayala, K. Morokuma, G.A. Voth, P. Salvador, J.J. Dannenberg, V.G. Zakrzewski, S. Dapprich, A.D. Daniels, M.C. Strain, O. Farkas, D.K. Malick, A.D. Rabuck, K. Raghavachari, J.B. Foresman, J.V. Ortiz, Q. Cui, A.G. Baboul, S. Clifford, J. Cioslowski, B.B. Stefanov, G. Liu, A. Liashenko, P. Piskorz, I. Komaromi, R.L. Martin, D.J. Fox, T. Keith, M.A. Al-Laham, C.Y. Peng, A. Nanayakkara, M. Challacombe, P.M.W. Gill, B. Johnson, W. Chen, M.W. Wong, C. Gonzalez, J.A. Pople, Gaussian 03, Revision C.02, Gaussian, Inc., Wallingford CT, 2004.
[38] M.E. Wieser, M. Berglung, Pure Appl. Chem. 81 (2009) 2131–2156.
[39] H.H. Jaffé, J. Am. Chem. Soc. 77 (1955) 4445–4448.
[40] R.W. Green, H.K. Tong, J. Am. Chem. Soc. 78 (1956) 4896–4900.
[41] P.O. Lumme, Suomen Kem. B30 (1957) 168–175.
[42] T. Khan, J.C. Halle, M.P. Simonnin, R. Schaal, J. Phys. Chem. 81 (1977) 587–590.
[43] M.S.K. Niazi, J. Mollin, Bull. Chem. Soc. Jpn. 60 (1987) 2605–2610.
[44] J.C. Hallé, J. Lelievre, F. Terrier, Can. J. Chem. 74 (1996) 613–620.
[45] B. Garcia, S. Ibeas, J.M. Leal, J. Phys. Org. Chem. 9 (1996) 593–597.
[46] P.I. Nagy, K. Takács-Novák, J. Am. Chem. Soc. 119 (1997) 4999–5006.
[47] H.P. Stephenson, H. Sponer, J. Am. Chem. Soc. 79 (1957) 2050–2056.
[48] J.F. Wojcik, T.H. Stock, J. Phys. Chem. 73 (1969) 2153–2157.
[49] F.H. Allen, Acta Crystallogr. B 58 (2002) 380–388.
[50] A. Kutoglu, C. Scheringer, Acta Crystallogr. C 39 (1983) 232–234.
[51] A. Jillavenkatesa, S.J. Dapkunas, L.-S.H. Lum, Particle Size Characterization, National Institute of Standards and Technology, Washington, 2001.
[52] M. Rehman, B.Y. Shekunov, P. York, P. Colthorpe, J. Pharm. Sci. 90 (2001) 1570–1582.
[53] R. Sabbah, S. Ider, Can. J. Chem. 77 (1999) 249–257.
[54] A. El Moussaoui, A. Chauvet, J. Masse, J. Therm. Anal. 39 (1993) 619–632.
[55] S.X. Wang, Z.C. Tan, Y.Y. Di, F. Xu, M.H. Wang, L.X. Sun, T. Zhang, J. Therm. Anal. Calorim. 76 (2004) 335–342.
[56] J.R. Allan, W.C. Geddes, C.S. Hindle, A.E. Orr, Thermochim. Acta 153 (1989) 249–256.
[57] G. Olofsson, Assignment of Uncertainties, in: S. Sunner, M. Månsson (Eds.), Experimental Chemical Thermodynamics, vol. 1, Pergamon Press, London, 1979 (Chapter 6).
[58] J.E. Hurst, B.K. Harrison, Chem. Eng. Commun. 112 (1992) 21–30.
[59] O. Ciocirlan, O. Iulian, J. Serb. Chem. Soc. 73 (2008) 73–85.
[60] B. Wunderlich, J. Therm. Anal. Calorim. 102 (2010) 413–424.
[61] C.M. Hansen, Hansen Solubility Parameters, second ed., CRC Press, Boca Raton, 2007.
[62] Y. Marcus, The Properties of Solvents, John Wiley, Chichester, 1998.
[63] C. Reichardt, Solvents and Solvent Effects in Organic Chemistry, third ed., Wiley-VCH, Weinheim, 2003.
[64] R. Todeschini, V. Consonni, Handbook of Molecular Descriptors, Wiley-VCH, Weinheim, 2000.
[65] D. Livingstone, Data Analysis for Chemists, Oxford University Press, Oxford, 1995.
[66] M. Baron, E.S. Arevalo, J. Chem. Educ. 65 (1988) 644–645.

View publication stats